An analytical model of the power spatial distribution for underwater optical wireless communication

Wei Wei[*], Zhang Xiao-hui, Chao Yue-yun, Zhou Xue-jun

Department of Weaponry Engineering, Naval University of Engineering,
No 717, Jiefang Avenue, Wuhan 430033, China

[*]Corresponding author: haijungong@qq.com

Employing optical propagation theory in Hankel transform, an analytical model of the optical power spatial distribution is derived for the ideal point optical source and the Gaussian laser, respectively. Experimental measurements of the spatial distribution of a Gaussian laser are presented. The expected results of our analytical model are in good agreement with experimental data.

Keywords: spatial distribution, optical wireless communication (OWC), Hankel transform, free-space optical (FSO) communication, underwater.

1. Introduction

Underwater vehicle to ship or buoy links enable the data to be transferred to a storage system for later analysis or to be transferred to shore or satellite by radio. In both cases, current acoustic technologies available in the commercial sector limit the channel bandwidth to a few tens of kilobits per second [1]. An optical link would allow large amounts of data to be transferred quickly and reliably between the surface and aquatic environment. Mobile networks of AUVs would also be possible with these links. A high bandwidth link (the recent published transfer rate has approached 1 Gbit/s [2]) of these networks would allow for sophisticated collaborative path planning and observation. Such a system could be employed for military uses, such as locating and disarming underwater mines or finding enemy submarines.

In short-range underwater applications, intensity modulation with direct detection (IM/DD) is mainly a practical transmission technique. The signal-to-noise ratio (SNR) of a direct-detection receiver is proportional to the square of the received optical power, implying that underwater links are susceptible to the optical power distribution [3]. Although volumetric Monte Carlo simulations have been used to provide uncompromised solutions to the distribution [4], it is difficult to simulate every scenario, since variables of the system should be accurately defined. The radiative transfer theory has been used to investigate the light propagation in random scattering media

accurately [5–9]. However, theoretical solutions to the radiative transfer equations (RTE) have been found to be difficult and excessively robust. Moreover, the underwater environment can be much more complex than the atmosphere due to the turbulence, subaquatic plants, the plankton, fishes, and the undulant seabed. So, having a model that would facilitate the evaluation of results would find wide application in practical scenarios. In previous works [10–13], exponential attenuation model was usually used as a simple approximation and model for practical scenarios, which describes the attenuation coefficient of water as the sum of absorption and scattering. But this approach is insufficient. JAGDISHLAL [14] experimentally proved that this model tends to magnify the attenuation of water scattering. As the development in fast Hankel transform (FHT) algorithms, employing optical propagation theory in Hankel transform would facilitate examination of the spatial domain effects of scattering on light underwater propagation and provide an analytical model.

To investigate the underwater optical power distribution, we start with a basic analysis of underwater optical propagation theory in Hankel transform. Then, an analytical model is provided for the ideal optical point source with simple approximations. A spatial distribution model for a Gaussian laser source is discussed next and experimental measurements of the spatial dispersion of the Gaussian laser source are finally presented.

2. Optical transfer theory in Hankel transform

For the line-of-sight underwater optical wireless communications applications, the geometry description of spatial power distribution is shown in Fig. 1, where an optical source is located at a distance $z = 0$. We are interested in computing the optical power distribution of this source on some plane perpendicular to the beam axis z where an optical receiver is located at a position r away from the beam axis. This power
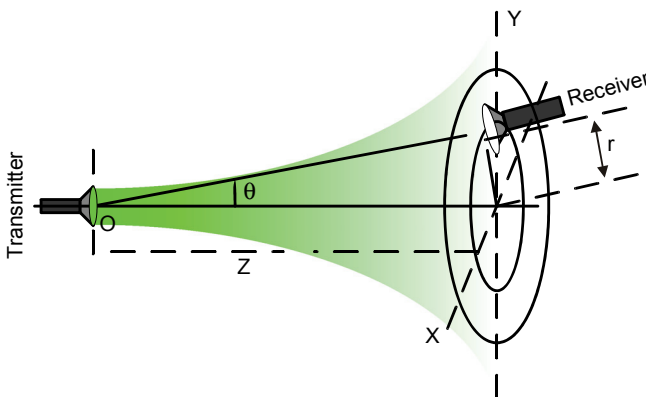

Fig. 1. Geometrical system in receiver plane.

distribution could also be obtained through the point spread function (PSF). Although computation of PSF requires solving a complex RTE, a small angle approximation (SAA) can be used so that the RTE can be solved analytically. The assumptions of the SAA include a forward-peaked scattering phase function (SPF), an axial symmetry on the plane of incidence, and no contribution from back-scattered light at distances $> z$ [15].

WELLS [16] convert the volume scattering function (VSF) to an image modulation transfer function so that the scattering properties can be calculated. MCLEAN [17, 18] and COCHENOUR *et al.* [19] simplified it by using the Hankel transform because of axial symmetry on the plane of incidence and introduced it into underwater OWC. It was given as [15–19]

$$F_w(S, z_r) = \exp\left\{-\int_0^{z_r}\left[a + b - bP\Big(S(z_r - z)\Big)\right]dz\right\} \tag{1}$$

where a is the absorption coefficient, b is the scattering coefficient, z_r is the propagation distance, S is the spatial domain frequency, $P(S)$ is the Hankel transform of the forward-peaked scattering phase function $p(\theta)$,

$$P(S) = \int_0^{\pi} p(\theta) J_0(\theta S) 2\pi\theta d\theta \tag{2}$$

where $J_0(\theta S)$ is the Bessel function of the first kind. Thus, the PSF $F_w(S, z_r)$ describes the effects of the water on the spatial domain properties of the propagating optical signal. If $f_0(r, z_r)$ is the optical power distribution of the transmitted light in free-space whose Hankel transform is $F_0(S, z_r)$, the optical power distribution in water is then given by [16]

$$f(r, z_r) = \frac{1}{2\pi}\int_0^{\infty} F_0(S, z_r) F_w(S, z_r) J_0(Sr) S \, dS \tag{3}$$

This is a general expression for all light sources. For long range, underwater environment is more complicated and shows varied scattering character such as the absorption coefficient, scattering coefficient, current velocity, temperature and the salinity of water. The long-range water could be divided into several short-range waters, and the corresponding PSF of each water column is labelled as $F_{w1}(S, z_r)$, $F_{w2}(S, z_r)$, $F_{w3}(S, z_r)$, ... Then the optical power distribution in water would be:

$$f(r, z_r) = \frac{1}{2\pi}\int_0^{\infty} F_0(S, z_r) J_0(Sr) S \, F_{w1}(S, z_r) F_{w2}(S, z_r) F_{w3}(S, z_r) \ldots dS \tag{4}$$

3. Spatial distribution for ideal point optical source

The spatial distribution for an ideal point optical source is the optical impulse response of water column in spatial domain. It describes the spatial domain effects from water scattering on light propagation. If the laser source $f_0(r, z_r)$ is an ideal point optical source, we have its Hankel transform

$$F_0(S, z_r) = 1 \tag{5}$$

For small S, we can expand $J_0(\theta S)$ in a Taylor series:

$$J_0(\theta S) = 1 - \frac{1}{4}(\theta S)^2 + \frac{1}{64}(\theta S)^4 \ldots \tag{6}$$

Substituting it into Eq. (2),

$$P(S) \approx 1 - \frac{1}{4}\langle \theta^2 \rangle S^2 \tag{7}$$

This allows arbitrary SPFs, only the quadratic term in S is retained in the small angle diffusion approximation. $\langle \ \rangle$ represents the expected value, and $\langle \theta^2 \rangle = = 2\pi \int_0^\pi \theta^2 p(\theta)\theta \mathrm{d}\theta$. In these limits we have the Hankel transform from Eq. (1)

$$F_w(S, z_r) \approx \exp(-az_r)\exp\left(-\frac{bz_r^3}{12}\langle \theta^2 \rangle S^2\right) \tag{8}$$

Substituting it and Eq. (5) into Eq. (3), the spatial distribution of an ideal point optical source in water is given as

$$f_{\mathrm{ideal}}(r, z_r) = \frac{\exp(-az_r)}{\frac{bz_r^3 \pi}{3}\langle \theta^2 \rangle}\exp\left(-\frac{r^2}{\frac{bz_r^3}{3}\langle \theta^2 \rangle}\right) \tag{9}$$

In this case, $f_{\mathrm{ideal}}(r, z_r)$ is a Gaussian probability density function for r with zero means and variances $bz_r^3\langle \theta^2 \rangle/6$. In Equation (9), $\exp(-az_r)$ is the absorption component, and the remaining is the scattered component. The analytical model suggests that it is a product of an exponential absorbing model and a scattering modified function which is Gaussian distribution. The pulse response is linked with the inherent optical properties a, b and $p(\theta)$ through Eq. (9). The mathematical simplicity of the model and the clarity with which inherent optical properties enter should appeal to theorists.

4. Spatial distribution for Gaussian laser source

In many practical underwater optical communication applications, laser sources are usually Gaussian distributed in free-space, whose optical power distribution in free-space at z with initial power P_0 is given by

$$f_0(r, z_r) = \frac{P_0}{2\pi V_0(z_r)} \exp\left\{-\frac{r^2}{2V_0(z_r)}\right\} \tag{10}$$

whose Hankel transform is given as

$$F_0(S, z_r) = P_0 \exp\left[-\frac{V_0(z_r)S^2}{2}\right] \tag{11}$$

where $V_0(z)$ is the variance of the Gaussian source in free-space, $\sqrt{V_0(z_r)} = z_r \tan(\omega)\pi$, here ω is the far field half-angle of divergence for Gaussian light source in free-space.

From among several SPFs, we choose the Gaussian SPF for its high accuracy [20]:

$$p(\theta) = \frac{1}{A\pi\theta_0^2} \exp\left(-\frac{\theta^2}{\theta_0^2}\right) \tag{12}$$

where $A = 2\pi \int_0^\pi 1/\pi\theta_0^2 \exp(-\theta^2/\theta_0^2)\sin(\theta)\,\mathrm{d}\theta$ is a normalized factor, and θ_0 is a characteristic scattering angle which has been experimentally tested by PETZOLD [21]. So, from Eqs. (2) and (12), we have

$$P(S) = \frac{2}{A} \exp\left[-\left(\frac{1}{2}\theta_0 S\right)^2\right] \tag{13}$$

Substituting $P(S)$ in Eq. (1) by Eq. (13) and after integration, it becomes

$$F_w(S, z_r) = \exp(-az_r)\exp(-bz_r)\exp\left[\frac{2b\,\mathrm{erf}\left(\frac{1}{2}\theta_0 S z_r\right)}{A\theta_0 S}\sqrt{\pi}\right] \tag{14}$$

where $\mathrm{erf}(x) = \dfrac{2}{\sqrt{\pi}}\int_0^x \exp(-t^2)\,\mathrm{d}t$.

Then, from Eqs. (3), (11) and (14), the optical power spatial distribution in water can be obtained,

$$f_{\text{Gaussian}}(r, z_r) = \frac{P_0 \exp(-az_r)}{2\pi} \times$$

$$\times \int_0^\infty \exp\left\{ -bz_r - \frac{1}{2}\left[\frac{b \operatorname{erf}(\theta_0 \pi S z_r)}{A \theta_0 S \sqrt{\pi}} - \frac{S^2}{\left[z_r \tan(\omega)\pi \right]^2} \right] \right\} J_0(Sr) S \, dS \tag{15}$$

In Equation (15), $\exp(-az_r)$ is the absorption component, and

$$\exp\left\{ -bz_r - \frac{1}{2}\left[\frac{b \operatorname{erf}(\theta_0 \pi S z_r)}{A \theta_0 S \sqrt{\pi}} - \frac{S^2}{\left[z_r \tan(\omega)\pi \right]^2} \right] \right\} \text{ is determined by the scat-}$$

tering coefficient b and the far field half-angle ω of divergence for Gaussian light source. Though Eq. (15) is not formally simple and cannot be evaluated explicitly, the FHT makes it much less time-consuming than methods mentioned in the first section and it is easy to predict various ranges and water environments. In the following section, this model will be experimentally verified as the light source used in our experiments is a Gaussian laser source.

5. Experiments design and results

Based on experimental results and *in situ* measurements, we can extract the basic feature of underwater scattering. The experimental setup is placed in a 20 m×5 m×1.2 m water pond, shown in Fig. 2. On one end, a continuous laser source (diode pumped solid state, Gaussian source in free-space, drive current 2 A, output power 200 mW, 532 nm, 3.5 mrad for far-field half-angle) was placed. At the opposite end an optical receiver, a Hamamatsu S5973 PIN was placed (photosensitive area 0.12 mm^2, photosensitive area diameter 0.4 mm, spectral response 0.28 AW^{-1} at 532 nm, dark current
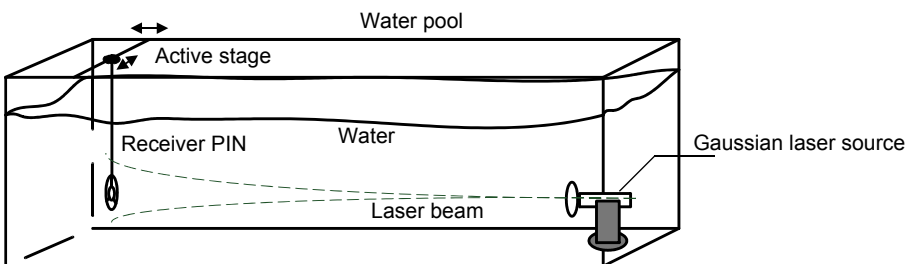

Fig. 2. Experimental setup in indoor pool (20 m×5 m×1.2 m).

maximum 0.1 nA). In an attempt to match the receiving characteristics imposed by the theoretical assumptions in the previous section, the PIN was placed on a motorized translation stage, maintaining an FOV that was as wide as possible (95°, full angle). A narrowband interference optical filter (Zolex JSL-25, central wavelength 540 nm, full width at half-maximum 15 nm, peak transmissivity ≥30%) was placed in front of the PIN, filtering ambient light.

A chlorophyll-based model given by HALTRIN [22] was employed by COCHENOUR *et al.* [19] and CHANCEY [11] to approach the scattering coefficient. However, this model, depending on the concentration of the scattering agents, is impractical in a 20 m×5 m×1.2 m pool. Based on the well-known formula with the dependence on volume scattering function, the scattering coefficient could be obtained by integrating scattering angle from 0 to π. This formula reproduces the experimental measurements of PETZOLD [21], who developed a general angular scattering meter to measure the volume scattering function of ocean water. From his data, the single scatter albedos (the rate of scattering efficiency to total attenuation b/c) were generally consistent for the same type of water, whose attenuation coefficients c vary just in a small span. Commercial environmental characterization optics (ECO) devices are available on Internet to survey VSF, but they are too expensive for us. In our case, we filled in the pond with artificial seawater, tap water mixed with industrial salt (sodium nitrite) of certain concentration. As our optical wireless communicating prototype was designed for offshore applications, we took Petzold's offshore experimental results as reference to carefully adjust the optical attenuation coefficient of the artificial seawater. When the attenuation coefficient was measured approximately 0.4 m^{-1} in the pool (which is 0.398 m^{-1} in Petzold's data), the single scatter albedo was assumed the same (0.551 m^{-1} in Petzold's data) and the scattering coefficient was 0.219 m^{-1}. Considering the single scatter albedo is determined by the scattering particles in nature, this is a big assumption and it is possible that the differences between our model and experiment are due to this incomplete characterization of the experimental conditions. But it is also extremely simple, and thus a convenient estimate.

The results in Fig. 3 have been normalized to the intensity received at z = 2 m when it is precisely aligned with the transmitted beam (position r = 0 mm). A general agreement is observed between experimental and theoretical results. Both results show that spatial dispersion increases with the increase of distance z. In contrast with large distances (z > 14 m), the optical spatial distributions for short distances (z < 14 m) retain much of the directionality that initial transmitted beam holds. When the transmitter (TX) and receiver (RX) are nearly aligned, the light is collected and the optical intensity attenuation is approximately 0.5 dB between 2 m and 3 m and also between 3 m and 4 m. As the RX deviates from the aiming axis, the optical power decreases rapidly while the optical intensities approach each other for different distances. For large distances (z > 14 m), the spatial dispersion of optical power is phanerous. The once highly directional characteristic of the transmitted laser light is lost. The optical intensity attenuation is approximately 0.2 dB between 5 m and 6 m and 0.1 dB between 6 m and 8 m when the receiver is accurately positioned. Furthermore, the optical
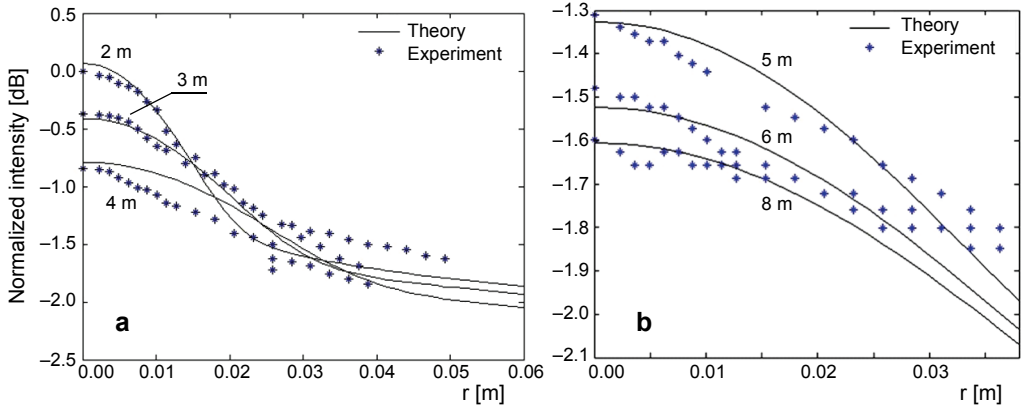
Fig. 3. Symmetry distribution for optical power at diverse (r, z), $\theta_0 = 0.13$ mrad [21], as far-field half-angle is 3.5 mrad, $V_0 = \tan(0.0035)z\pi$: distances of 2, 3 and 4 m (**a**), distances of 5, 6 and 8 m (**b**).
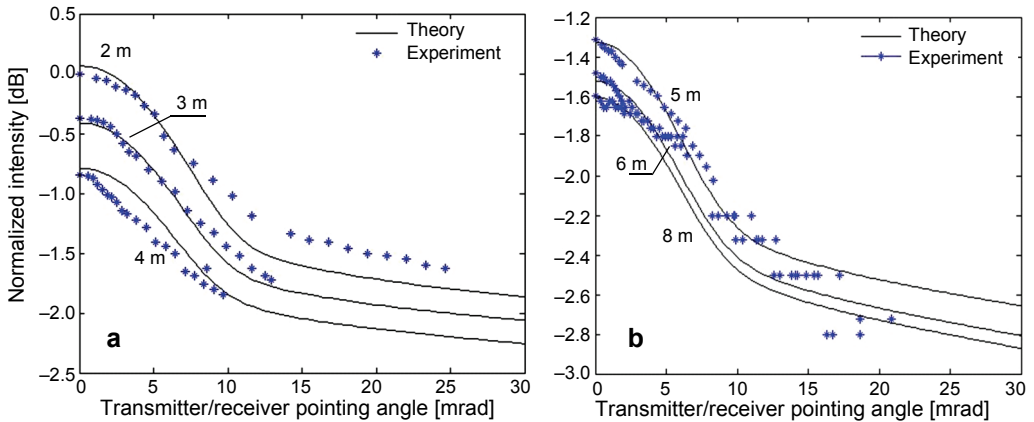

Fig. 4. The normalized intensity vs. TX/RX pointing angle: distances of 2, 3 and 4 m (**a**), distances of 5, 6 and 8 m (**b**).

power fades tardily when the alignment deflection increases. This may be attributed to the dominance of multiple-scattering and diffused photos at large distances. The theory and experimental data are also presented as the intensity versus TX/RX pointing angle. From Figure 4, optical intensity presents distinct forward scattering characters for various distances. For a given TX/RX pointing angle, the intensity decreases when the distance increases. And the larger the distance becomes the slower the intensity decays. This gives us an insight into the beam dispersion in the spatial distribution of the light in water. The results could explained how the water volume scattering effects optical communication applications. When the distance is relatively short ($z < 14$ m), the RX and TX should be accurately aligned because a slight deviation from the aiming axis would induce a significant reduction in received optical

power and lead to a link-break in the communication. When the distance is relatively long, there is a deviation tolerance for the RX /TX position and the alignment is less critical because the loss of power is relatively small for a mild excursion, but this tolerance costs a higher overall loss in optical power. Those results inspire us that if the distribution of light source could be adjusted by a controllable optical system, the distribution of optical power in water would be rebuilt according to the TX/RX position and the communication link should be more robust in complicated underwater environments.

6. Summary

In this paper, we investigate the characteristics of spatial optical power distribution for underwater light propagation which strongly affects power budget in underwater wireless optical communication. An analytic spatial domain response function model for an ideal optical impulse is deduced, which is suggested to be a Gaussian distribution. The mathematical simplicity of the model and the clarity of its inherent optical properties makes it an attractive analytical tool for general problems in the spatial domain effects of multiple scattering in water. A computer analytic model for Gaussian laser source was also developed using Hankel transform of PSF simplified with SAA. The expectation of this model overall agrees with laboratory experimental data. The validation between model and experiment confirms that the directionality of the laser beam is lost as particulates in the environment broaden the intensity distribution faster than the divergence of the laser source itself. In our earlier paper [3], considering the geometrical wastage induced by receiver size, spatial position and receiving angle, the receiving optical power was obtained based on the distribution, and we implemented an experimentation in a pool which verified that our method achieved a better agreement with experimental data than the exponential attenuation model.

References

[1] AKYILDIZ I.F., POMPILI D., MELODIA T., *Underwater acoustic sensor networks: Research challenges*, Ad Hoc Networks **3**(3), 2005, pp. 257–279.

[2] HANSON F., RADIC S., *High bandwidth underwater optical communication*, Applied Optics **47**(2), 2008, pp. 277–283.

[3] WEI W., ZHANG X.H., RAO J.H., *Study on computing the receiving optical power in underwater optical wireless communication*, Chinese Journal of Lasers **38**, 2011, article 0905002.

[4] JAFFE J.S., *Monte Carlo modeling of underwater-image formation: Validity of the linear and small-angle approximations*, Applied Optics **34**(24), 1995, pp. 5413–5421.

[5] WEI WEI, XIAOHUI ZHANG, JIONGHUI RAO, WENBO WANG, *Time domain dispersion of underwater optical wireless communication*, Chinese Optics Letters **9**(3), 2011, article 030101.

[6] JARUWATANADILOK S., *Underwater wireless optical communication channel modeling and performance evaluation using vector radiative transfer theory*, IEEE Journal on Selected Areas in Communications **26**(9), 2008 , pp. 1620–1627.

[7] SWANSON N.L., GEHMAN V.M., BILLARD B.D., GENNARO T.L., *Limits of the small-angle approximation to the radiative transport equation*, Journal of the Optical Society of America A **18**(2), 2001, pp. 385–391.

[8] ISHIMARU A., KUGA Y., CHEUNG R.L.-T., SHIMIZU K., *Scattering and diffusion of a beam wave in randomly distributed scatterers*, Journal of the Optical Society of America **73**(2), 1983, pp. 131–136.

[9] SANCHEZ R., MCCORMICK N.J., *Analytic beam spread function for ocean optics applications*, Applied Optics **41**(30), 2002, pp. 6276–6288.

[10] JIANQI SHEN, HAITAO YU, JINDENG LU, *Light propagation and reflection-refraction event in absorbing media*, Chinese Optics Letters **8**(1), 2010, pp. 111–114.

[11] CHANCEY M.A., *Short Range Underwater Optical Communication Links*, Master Thesis, North Carolina State University, 2005, pp. 30–31.

[12] VASILESCU, *Data Collection, Storage, and Retrieval with an Underwater Sensor Network*, Proceedings of ACM, SenSys'05, November 2–4, 2005, San Diego, California, USA, p. 154.

[13] ARNON S., *Underwater optical wireless communication network*, Optical Engineering **49**(1), 2010, article 015001.

[14] JAGDISHLAL G.Y., *Underwater Free Space Optics*, Master Thesis, North Carolina State University, 2006, pp. 41–57.

[15] MULLEN L., *Optical propagation in the underwater environment*, Proceedings of SPIE **7324**, 2009, article 732409.

[16] WELLS W.H., *Loss of resolution in water as a result of multiple small-angle scattering*, Journal of the Optical Society of America **59**(6), 1969, pp. 686–691.

[17] MCLEAN J.W., VOSS K.J., *Point spread function in ocean water: Comparison between theory and experiment*, Applied Optics **30**(15), 1991, pp. 2027–2030.

[18] MCLEAN J.W., FREEMAN J.D., WALKER R.E., *Beam spread function with time dispersion*, Applied Optics **37**(21), 1998, pp. 4701–4711.

[19] COCHENOUR B.M., MULLEN L.J., LAUX A.E., *Characterization of the beam-spread function for underwater wireless optical communications links*, IEEE Journal of Oceanic Engineering **33**(4), 2008, pp. 513–521.

[20] MOORADIAN G.C., GELLER M., STOTTS L.B., STEPHENS D.H., KRAUTWALD R.A., *Blue-green pulsed propagation through fog*, Applied Optics **18**(4), 1979, pp. 429–441.

[21] PETZOLD T.J., *Volume Scattering Functions for Selected Ocean Waters*, SIO Ref. 72-78, Scripps Institution of Oceanography, California, San Diego, 1972, pp. 36, 46.

[22] HALTRIN V.I., *Chlorophyll-based model of seawater optical properties*, Applied Optics **38**(33), 1999, pp. 6826–6832 .